Elucidation of Intermediate (Mobile) and Slow (Solidlike) Protein Motions in Bovine Lens Homogenates by Carbon-13 NMR Spectroscopy†

Courtney F. Morgan,‡ Thomas Schleich,*,‡ G. Herbert Caines,‡ and Patricia N. Farnsworth§

Department of Chemistry, University of California, Santa Cruz, California 95064, and Department of Physiology, New Jersey Medical School, Newark, New Jersey 07103

Received October 24, 1988; Revised Manuscript Received February 14, 1989

ABSTRACT: The motional dynamics of lens cytoplasmic proteins present in calf lens homogenates were investigated by two ^{13}C nuclear magnetic resonance (NMR) techniques sensitive to molecular motion to further define the organizational differences between the cortex and nucleus. For the study of intermediate (mobile) protein rotational reorientation motion time scales [rotational correlation time (τ_0) range of 1–500 ns], we employed ^{13}C off-resonance rotating frame spin–lattice relaxation, whereas for the study of slow (solidlike) motions ($\tau_0 \geq 10$ μs) we used the solid-state NMR techniques of dipolar decoupling and cross-polarization. The frequency dependence of the peptide bond carbonyl off-resonance rotating frame spectral intensity ratio of the lens proteins present in native calf nuclear homogenate (42% protein) at 35 °C indicates the presence of a polydisperse mobile protein fraction with a $\tau_{0,eff}$ (mean) value of 57 ns. This mean value is consistent with the average value calculated from the known water-soluble nuclear lens protein polydispersity assuming a cytoplasmic viscosity 3 times that of pure water. Lowering the temperature to 1 °C, a temperature which produces the cold cataract, results in an overall *decrease* in $\tau_{0,eff}$ to 43 ns, suggesting a selective removal of β_H-, LM-, and possibly γ_S-crystallins from the mobile lens protein population. The presence of solidlike or motionally restricted protein species was established by dipolar decoupling and cross-polarization. The fraction of motionally restricted protein in the nuclear region varied from 0.35 to 0.45 in the temperature range of 35–1 °C. For native cortical homogenate (25% protein), the off-resonances rotating frame spectral intensity ratio frequency-dependent curves for the protein carbonyl resonance yielded $\tau_{0,eff}$ values of 34 and 80 ns at 35 and 1 °C, respectively. Both values were reconciled with the known lens cortex soluble protein polydispersity using an assumed cytoplasmic viscosity 1.5 times that of pure water at the same temperature. Comparison of proton dipolar-decoupled and nondecoupled ^{13}C NMR spectra of native cortical homogenate at 20 °C indicates the absence of significant contributions from slowly tumbling, motionally restricted species. This interpretation was confirmed by the failure to detect significant lens protein ^{13}C–^{1}H cross-polarization at this temperature. However, at 1 °C, the fraction of solidlike protein was 0.15. Concentrated cortical homogenates at 20 °C (42% protein), by contrast, gave cross-polarization spectra with maximum absolute signal intensities 50–70% of native nuclear homogenates, but with similar magnetization parameters. These studies establish the presence of both mobile and solidlike protein phases in calf lens nuclear homogenate, whereas for the native cortical homogenate, within the detection limits of NMR, the protein phase is mobile, except at low temperature where a small fraction of solidlike protein phase is present.

The molecular basis of lens transparency is ultimately dependent upon the spatial order of the high concentrated cytoplasmic proteins, the α-, β-, and γ-crystallins. Lens opacification, the medical condition of cataract, occurs following loss of this order, concomitant with the occurrence of enhanced light scattering. For the lens cortex, Delaye and Tardieu (1983) have argued that transparency is dependent upon short-range spatial order established by the high packing density of the constituent cytoplasmic proteins.

In this study, the motional dynamics of the cytoplasmic lens proteins are investigated by the use of two nuclear magentic resonance (NMR)[1] techniques sensitive to molecular motion to further define the organizational differences between the cortex, the outer portion of the lens, and the more inert central nuclear region. The cortex consists of cells that are the product of the differentiation of the epithelial cells which cover the anterior lens face. These cells elongate to form successive cellular lamellae throughout life. They are metabolically active and exhibit active protein synthesis. With time, they lose their nuclei and most organelles, and are displaced inward. With inward displacement, a number of alterations occur to form the nuclear region.

The rationale for this investigation is based on the considerable evidence for organizational differences in these two lens regions. For example, the three-dimensional architecture of the cytoplasmic matrix as visualized by high-voltage electron microscopy suggests a more ordered molecular organization in the nucleus (Farnsworth et al., 1980); the nucleus is significantly dehydrated (Philipson & Fagerholm, 1973; McEwan & Farnsworth, 1987); water diffusion is 2–3 times slower in the nucleus than in the cortex (Neville et al., 1974; Haner et

† This work was supported by National Institutes of Health Grants EY 04033 and EY 05787.

‡ University of California.

§ New Jersey Medical School.

[1] Abbreviations: NMR, nuclear magnetic resonance; QELS, quasi-elastic light scattering; CP, cross-polarization; CP/MASS, cross-polarization/magic angle sample spinning; FID, free induction decay; RF, radiofrequency; CSA, chemical shift anisotropy; NMRD, nuclear magnetic resonance dispersion; Me, methyl.

0006-2960/89/0428-5065$01.50/0

al., 1989); resistivity, which is dependent in part on ion mobility, is greater in the nucleus by at least a factor of 2 (McEwan & Farnsworth, 1987); protein concentration increases as nuclear fibers form (Philipson & Fagerholm, 1973); with time, a progressive conversion of the soluble protein fraction to an insoluble form occurs in the nucleus (Zigler & Goosey, 1981); finally, the proteins synthesized during development of the lens are different in composition than those synthesized in the adult (Carper et al., 1985), and, therefore, the initial composition of the central region of the nucleus is different from the adult cortex.

In this investigation, we employ two NMR techniques for the study of intermediate [correlation time (τ_0) of 10^{-9}–10^{-6} s] and slow ($\tau_0 > 10^{-5}$ s) protein molecular motion time scales in lens homogenates: ^{13}C rotating frame spin–lattice relaxation in the presence of an off-resonance radio-frequency field (James et al., 1977, 1978, 1979) is employed for the detection of mobile macromolecular species, and the presence of solidlike structural elements is detected by the solid-state double-resonance NMR techniques of dipolar decoupling and cross-polarization [for reviews, see Yannoni (1982) and Lyerla et al. (1982)].

The NMR techniques utilized in this study of lens protein motional dynamics offer information complementary to that afforded by QELS applied previously to the lens. Both techniques are sensitive to molecular motion. QELS yields a correlation time(s) from which a translational mutual diffusion coefficient is calculated. The off-resonance rotating frame relaxation technique, by contrast, provides a *rotational* correlation time. Solid-state NMR techniques furnish evidence for the occurrence of slow solidlike ($\tau_0 > 10^{-5}$ s) molecular motions.

The NMR studies presented in this paper provide evidence for the occurrence in lens nuclear homogenates of an isotropically mobile phase of protein and a solidlike phase, possibly a gel, whereas for cortical homogenate, essentially all of the lens protein behaves as an isotropically mobile phase at physiologically relevant temperatures.

THEORY

The theoretical formalism relating the off-resonance rotating frame spin–lattice relaxation time ($T_{1\rho}^{off}$) to molecular motion has been described by James and co-workers (James et al., 1977, 1978, 1979; Schleich et al., 1989). The pulse sequence consists of the application of a low-power off-resonance ^{13}C radio-frequency field for a time period of no less than 3 times the spin–lattice relaxation time (T_1) followed by a 90° ^{13}C observe pulse to assess the steady-state magnetization established along the effective field (B_{eff}). The effective magnetization (M_{eff}) is given by $M_{eff} = M_0 T_{1\rho}^{off}/T_1$, where M_0 is the thermal equilibrium magnetization along B_0. The ratio (R) of the ^{13}C signal intensity in the presence of an off-resonance field to the intensity obtained in the absence of the field is given by M_{eff}/M_0 ($=T_{1\rho}^{off}/T_1$). This spectral intensity ratio is related to the correlation time for rotational tumbling (τ_0) by means of appropriate spectral density functions (James et al., 1978; James, 1984; Schleich et al., 1989). Plots of R vs τ_0 at different values of the off-resonance frequency and the frequency dependence (dispersion) of R with the Larmor precessional frequency in the effective magnetic field, ω_e, for different values of τ_0, assuming a monodisperse isotropically tumbling population of particles, have been previously presented (Schleich et al., 1989). In the original formalism developed by James and co-workers, only contributions from dipolar relaxation were assumed to occur, as was monodispersity of the spherical tumbling particles. Because the present experiments were conducted at a much higher B_0 value (7.05 T), we have extended the formalism to include relaxation contributions from chemical shift anisotropy and the effects of polydisperse mixtures (Schleich et al., 1989).

For solidlike materials ($\tau_0 \geq 10^{-5}$ s), the magnetic dipole–dipole interactions do not motionally average to zero, and the dominant source of line broadening in a ^{13}C NMR spectrum arises from protons located in the immediate vicinity of the ^{13}C nucleus [for a review, see Yannoni (1982)]. These nearby protons generate a substantial local magnetic field (B_z^H) which either adds or subtracts to the external field B_0, thus causing significant upfield or downfield chemical shift changes in the ^{13}C resonance frequency resulting in very broad (kilohertz) resonant line widths, too broad for detection. Two different approaches to achieve resonance signal narrowing are utilized in this study. The first is the application of a high-power proton decoupling field such that $\gamma_H B_{2H}/2\pi \gg \Delta\nu_{HH}$ ($\gamma B_2/2\pi \approx 30$–$60$ kHz), i.e., dipolar decoupling, resulting in the removal of the static ^{13}C–^1H dipolar interaction (Bloch, 1958; Pines et al., 1973; Gerstein & Dybowski, 1985), which contributes in part to the broad spectral line shapes observed for solidlike samples. The second method, cross-polarization of magnetization under Hartmann–Hahn (1962) match conditions from abundant proton spins to rare ^{13}C spins (Pines et al., 1973; Gerstein & Dybowski, 1985), results in a proton-enhanced ^{13}C resonance signal only from those ^{13}C and ^1H spins which have a nonvanishing static dipolar interaction, i.e., from motionally restricted (solidlike, $\tau_0 \geq 10^{-5}$ s) molecular species.

Thus, the application of a scalar decoupling irradiation field ($\gamma_H B_{2H}/2\pi \approx 3$ kHz) permits detection of isotropically mobile species; the dipolar decoupled spectrum [irradiation field strengths of at least 8–10 G (34–43 kHz)] contains resonances from both motionally narrowed and motionally restricted species, whereas the cross-polarization spectrum (obtained in the presence of dipolar decoupling) only contains contributions from motionally restricted species. Comparison of the integrated spectral intensity for a dipolar-decoupled with the corresponding scalar proton-decoupled ^{13}C spectrum permits the assessment of the fraction of motionally restricted species (nuclear spins) provided that the repetition time for spectral accumulation is sufficiently long to allow the z magnetization of both the mobile and solidlike species to recover their thermal equilibrium values and that significant nuclear Overhauser effects are absent. The latter assumption is realistic given the correlation times of the lens proteins. In addition, chemical shift anisotropy of the carbonyl carbon and static dipolar ^{13}C–^{14}N coupling lead to resonance line broadening of motionally restricted ($\tau_0 \geq 10^{-5}$ s) peptide backbone ^{13}C carbonyl carbons (Torchia & VanderHart, 1979). The former can be removed by magic angle spinning, a technique not employed in this study.

The increase of spectral intensity in a CP experiment is governed by the cross-polarization transfer rate (T_{IS}^{-1}) which in turn is dependent upon the second moment of the IS (^{13}C–^1H) dipolar interaction (Demco et al., 1975; Gerstein & Dybowski, 1985). In the absence of interactions other than dipolar, the second moment is proportional to r_{IS}^{-6}. The decay of carbon polarization mirrors the decline in proton magnetization which is governed by $T_{1\rho}(^1H)$ in the CP experiment (Schaefer et al., 1977; Gerstein & Dybowski, 1985). The intensity of a CP spectral band is dependent primarily on the spin–lattice relaxation time of the protons in the rotating frame [$T_{1\rho}(^1H)$] and the cross-polarization transfer time (T_{CH}). Both $T_{1\rho}(^1H)$ and T_{CH} are dependent upon molecular motion. Optimum CP signal intensity is attained when $T_{1\rho}(^1H) >$ CP

contact time > T_{CH}. Thus, changes in molecular dynamics are reflected in altered CP spectral intensities.

The magnetization transfer kinetic parameters governing polarization transfer between ^1H and ^{13}C nuclei can be obtained by varying the CP contact time. Magnetization transfer theory is well worked out (Mehring, 1983). Difficulties associated with the determination of kinetic parameters from variable CP contact time data have been noted (Earl et al., 1987; Alemany et al., 1983).

This magnetic resonance strategy, utilizing solid-state techniques, is very similar to that employed by Sutherland et al., (1979) for the successful study of hemoglobin S gelation in concentrated protein solutions and the intact red blood cell.

Experimental Procedures

Nuclear Magnetic Resonance Measurements. All measurements were made at 7.05 T using a General Electric GN-300 spectrometer equipped with a broad-band decoupler and Chemagnetics accessories to permit high-power ^{13}C–^1H double-resonance experiments. The $T_{1\rho}^{off}$ experiment was performed using a 20-mm broad-band probe as previously described (James et al., 1978; Schleich et al., 1989). The broad-band decoupler was used to provide the off-resonance B_1 field. Calibration of the off-resonance B_1 field was achieved by determining the nutational frequency of the broad-band decoupler output at a given power level on a standard sample. The standard sample contained 2% (w/v) 1-^{13}C-enriched sodium acetate (99 atom %) adjusted to the appropriate ionic strength with NaCl and ca. 35 μM $MnCl_2$ to reduce the carbonyl ^{13}C T_1 to ~6.5 s. The probe tune varied somewhat from the standard to the sample of interest but could be compensated for with slight adjustment of the tune capacitor. The coil quality factor ("Q") did not change significantly upon replacing the standard with the sample. In most experiments, the ^{13}C off-resonance field strength was ca. 0.5 G; off-resonance frequencies ranged from 2 to 36 kHz from the carbonyl resonance. All off-resonance rotating frame spectra were referenced against a control spectrum acquired at a resonance offset of 200 kHz. Typically, spectra were taken with sweep widths of ±15 kHz and 4K data points. Quadrature phase detection and phase cycling to remove base-line artifacts were used. Between acquisitions, the off-resonance field was continuously applied for approximately $3T_1$ (8–18 s) of the protein carbonyl resonance. Sample temperature was regulated to within ±0.5 °C of the desired value.

Three kinds of ^{13}C–^1H double-resonance experiments were performed: dipolar-decoupled, scalar-decoupled, and proton-enhanced cross-polarization. Initial experiments utilized a Chemagnetics Double Resonance CP/MASS probe which was used without sample spinning. Glass NMR sample tubes (8-mm o.d.) were employed for these measurements. The sample temperature was maintained within ±1 °C of the desired value. For the dipolar-decoupled experiments and subsequent CP experiments, a ^{13}C–^1H double-resonance high-power probe was constructed. A modified design (R. Wittebort, personal communication) similar to that devised by Jiang et al. (1987) was adapted for use at 7.05 T. A GE GN-300 blank probe body was modified to allow for installation of high-power RF circuitry. Components were chosen for minimal losses at high power levels. The 75.45- and 300.1-MHz leads were made of low-loss, semirigid coaxial tubing (0.25-in. diameter) (Precision Tubes) and matched connectors (Omnispectra). The $\lambda/4$ filter on the high-frequency side of the coil utilized air-articulated, semirigid coaxial tubing (0.5-in. diameter) (Precision Tubes). Variable capacitors were of nonmagnetic design (Voltronics), while the fixed-chip capacitors employed were designed for low losses at high frequencies and voltages (American Technical Ceramics).

The uppermost portion of the probe consisted of a sample chamber contained within a glass dewar which allowed sample temperature regulation within ±1.0 °C using the standard GN-300 variable-temperature controller unit; 12-mm glass NMR sample tubes were used.

For a 10 mm long, 12-mm diameter solenoidal coil, a 10-μs ^{13}C 90° pulse width was obtained at a power input of 200 W with a sample of adamantane. Coil "Q's" were determined on a loaded coil (adamantane) at room temperature: $Q(^{13}C)$ = 190; $Q(^1H)$ = 470.

The dipolar-decoupled and scalar-decoupled experiments consisted of a τ–90° pulse sequence. High- (dipolar decoupled) and low- (scalar decoupled) level ^1H irradiation during acquisition of the FID was employed. A ^{13}C 45° tipping pulse (5 μs), a sweep width of ±20 kHz (quadrature phase detection), 2K data points (acquisition time = 25.6 ms), and a 4.025-s repetition time were used. An 8-G ($\gamma_2B_2/2\pi$ = 34 kHz) ^1H irradiation field was applied during the acquisition of the ^{13}C FID (dipolar decoupling) whereas an 0.8-G ($\gamma_2B_2/2\pi$ = 3.4 kHz) irradiation field was employed for scalar decoupling. ^{13}C spin–lattice relaxation times were estimated for the cross-polarizable material in nuclear homogenate samples by using the T1CP method of Torchia (1978). The inversion recovery method was used to estimate ^{13}C T_1 values for the mobile protein species following procedures previously described (Matson et al., 1984).

Cross-polarization spectra were obtained by establishing the Hartmann–Hahn condition ($\gamma_1B_1 = \gamma_2B_2$) on a sample of adamantane. The proton and carbon channels were carefully tuned to maximize and minimize the forward and reflected power, respectively. The ^{13}C transmitter power was varied at fixed ^1H irradiation power until the best match was obtained as manifested by a maximum in the CP spectral intensity. This was followed by optimization of the 90° ^1H preparation pulse duration. Typical match conditions were the following: ^{13}C, 500 W, B_1 = 33.4 G; ^1H, 400 W, B_1 = 8.4 G. Alternation of the proton spin temperature was used to suppress unwanted signal intensity (Stejskal & Schaefer, 1975). Data were collected with a 180° phase shift after each scan. More recent CP experiments employed phase cycling after every second scan with superior artifact suppression (Stejskal & Schaeffer, 1975). Contact times varied from 7.5 μs to 3 ms, and a repetition time of 2 s was used. No delay to permit dipolar dephasing was imposed between the termination of the contact period and the start of the acquisition of the dipolar-decoupled ^{13}C FID. The proton channel tune and match were optimized to each experimental sample.

Spectra were calibrated by using the chemical shifts of adamantane (Earl & VanderHart, 1982). Methyl, α, β, and carbonyl carbon band assignments follow those presented for elastin from intact calf ligamentum nuchae fibers (Torchia & VanderHart, 1979).

Data Analysis. Off-resonance rotating frame relaxation spectra were analyzed by determining the carbonyl resonance band intensity using the GE NMR GEM software integration routine. The spectral band intensities at each offset were then divided by the reference area obtained far off-resonance to yield an intensity ratio. The intensity ratios from the dispersion data were then fit to relaxation models (Schleich et al., 1989) by using nonlinear least-squared methods (Daniel & Wood, 1980) to obtain mean values of the rotational correlation time ($\tau_{0,eff}$).

Line-shape deconvolution using the GE NMR GEMCAP routine was employed to obtain relative resonance band areas in the case of overlapping resonances. Typically, three of four bands were fit to the CP aliphatic signal from lens homogenates and gel samples. The fits were constructed with lines consisting of 70% Gaussian and 30% Lorentzian character. In each case, the RMS error was minimized.

The spectral data obtained from variable CP contact time experiments were fit to eq 1 to obtain magnetic cross-polarization kinetic transfer parameters (Earl et al., 1987) where

$$H = H_0 \frac{\exp[-t_c/T_{1\rho}(^1\mathrm{H})] - \exp(t_c/T_{\mathrm{CH}})}{1 - T_{\mathrm{CH}}/T_{1\rho}(^1\mathrm{H})} \quad (1)$$

H is the observed signal intensity, H_0 is the theoretical maximum signal intensity in the absence of $T_{1\rho}(^1\mathrm{H})$ relaxation, t_c is the CP contact time, and T_{CH} is the cross-polarization transfer time between $^1\mathrm{H}$ and $^{13}\mathrm{C}$. The fitting was performed by using nonlinear least-squares methods (Daniel & Wood, 1980).

Lens Homogenates. Calf lens material was prepared from calf eyes obtained from a nearby slaughterhouse. Lenses were removed under sterile conditions by way of a 270° incision on the anterior portion of the globe circumscribing the iris. Concomitant with slight pressure on the globe, a small nick was made in the lens capsule resulting in lens expulsion and decapsulation. The lenses were cooled to visualize the nuclear–cortical boundary, which was followed by dissection to separate the two lens components.

Cortical homogenates were prepared with a glass hand-operated tissue homogenizer at ice bath temperature. The homogenate was centrifuged at 8000*g* and 4 °C for 2 h. The less dense upper layer was discarded. The nuclear material was homogenized with a motorized Teflon ball tissue homogenizer at ice bath temperature. No time-dependent changes in the NMR behavior of either homogenate preparation were observed.

The protein concentration of cortical and nuclear homogenate samples was varied by dehydration and dilution, respectively. Cortical homogenate was concentrated by using a vacuum centrifuge (Sorval Spin-vac) to 42% protein relative to the native value of 25%. Nuclear homogenates were diluted with distilled water to 22% and 31% protein compared to the 42% native value. Protein concentration was determined by oven drying to constant weight and assuming dry weight to be due entirely to protein.

Polyacrylamide Gels. The synthesis of polyacrylamide gels followed published methods (Tanaka, 1978). After a 1-h curing period, the gels were removed from the glass tubes and placed in a deoxygenated water "stop" bath for 4 h. The gels were then soaked in distilled water with at least three changes over 24 h to remove any unreacted monomer. Soak baths were at least 10 times the volume of the gel. Gels were stored in H_2O at 4 °C.

Results

Nuclear Homogenate. The off-resonance rotating frame spin–lattice relaxation spectral intensity ratio frequency-dependent (dispersion) curves for the carbonyl resonances of native nuclear homogenate lens proteins (42% protein) at 35 and 1 °C are shown in Figure 1. Preliminary $^{13}\mathrm{C}$ T_1 measurements indicate a maximum value of ca. 6 s for the carbonyl carbon of proteins present in lens homogenates under the conditions employed in this study. The fitted curves, using a monodisperse, isotropically tumbling protein system model [dashed ($\tau_{0,\mathrm{eff}}$ = 57 ns) and solid ($\tau_{0,\mathrm{eff}}$ = 43 ns) lines], do not

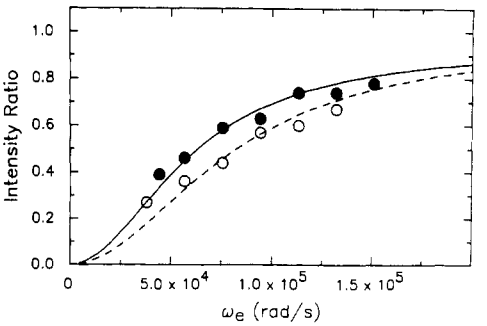

FIGURE 1: Carbonyl $^{13}\mathrm{C}$ intensity ratio (R) vs ω_e plots for calf lens nuclear homogenate proteins at 35 °C (○) and 1 °C (●). The latter temperature induces a phase transition resulting in a "cold cataract", characterized by intense light scattering (opacification). The solid and dashed lines represent the best-fit lines obtained by nonlinear regression assuming a model of monodisperse isotropic reorientation with $\tau_{0,\mathrm{eff}}$ values of 43 and 57 ns, respectively. Spectral acquisition parameters are noted under Experimental Procedures.

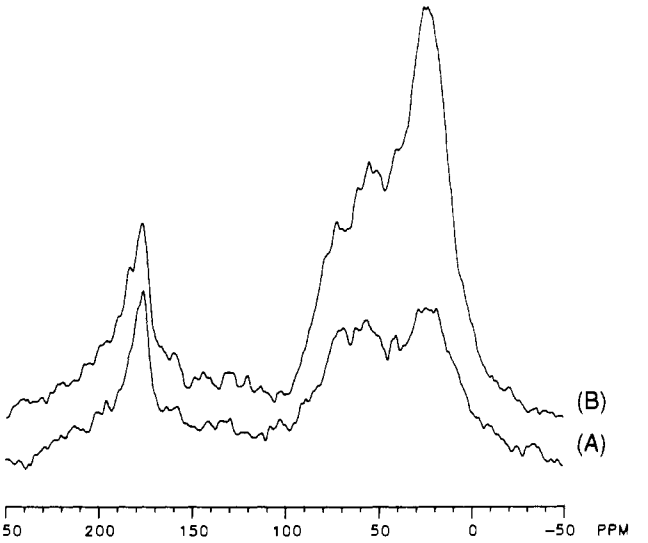

FIGURE 2: Comparison of $^{13}\mathrm{C}$ NMR spectra of calf lens nuclear homogenate lens proteins acquired in the presence and absence of proton dipolar decoupling at 1 °C. (A) Scalar decoupled; (B) dipolar decoupled. Spectral acquisition parameters are noted under Experimental Procedures. Number of accumulations = 512. A line-broadening factor of 150 Hz was applied to the FID prior to Fourier transformation.

quite attain the asymptotic limiting value of 1.00; values of 0.97 and 0.94 were obtained at 35 and 1 °C, respectively. This discrepancy is most likely a manifestation of lens protein polydispersity and/or the consequence of the monodisperse model employed in the fits. In contrast to the 2.7-fold *increase* expected for τ_0 upon reducing the temperature from 35 to 1 °C (the viscosity of pure water at each temperature was assumed), the lower temperature of 1 °C, produced an overall *decrease* in τ_0. Since this temperature supports the cold cataract phase transition, the observed decrease undoubtedly reflects the selective removal of higher molecular weight nuclear lens proteins into an NMR-invisible pool (which requires high-power solid-state NMR techniques for spectral visualization).

In nuclear homogenates, a significant solidlike protein fraction is indicated by an increase in $^{13}\mathrm{C}$ resonance signal intensity concomitant with dipolar decoupling compared to spectra taken with scalar decoupling, i.e., without dipolar decoupling (Figure 2). The approximate fractions (in terms of the number of nuclear spins) of solidlike phase, i.e., displaying restricted motion, are 0.35, 0.42, and 0.45 at 35, 20, and 1 °C, respectively. Preliminary spin–lattice (T_1) relaxation

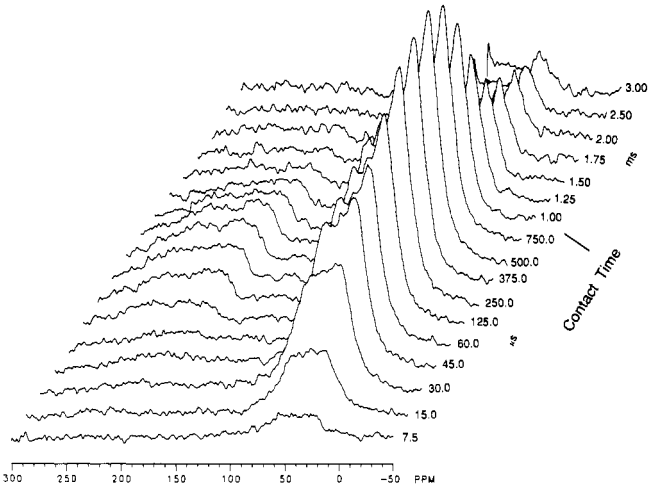

FIGURE 3: Cross-polarization ^{13}C NMR spectra of calf lens nuclear homogenate proteins recorded at 20 °C as a function of the cross-polarization contact time. Spectra acquisition parameters are noted under Experimental Procedures. Number of accumulations = 3000. A line-broadening factor of 150 Hz was employed.

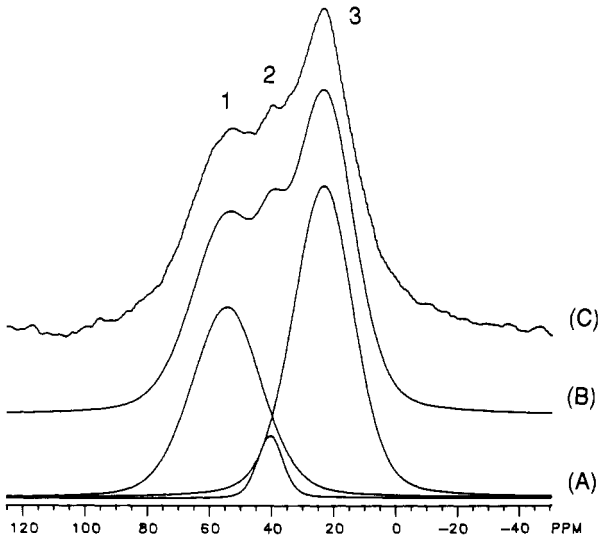

FIGURE 4: Spectral line-shape deconvolution and resonance assignments (1, C_α; 2, C_β; 3, C-methyl) of the aliphatic region in the cross-polarization spectra of lens nuclear homogenate proteins shown in Figure 4. (A) Individual component resonances; (B) calculated spectrum; (C) experimental spectrum.

time estimations for the aliphatic carbons present in the cross-polarizable material (solidlike) of a nuclear homogenate indicate a maximum value of ca. 2.3 s under the temperature conditions employed in this study, whereas the corresponding value for the mobile fraction is ca. 2.0 s. Thus, measurements of solidlike protein content were performed at a repetition time of 6.025 s to minimize T_1 discrimination induced artifacts.

CP experiments performed on nuclear homogenates at 1, 20, and 32 °C confirm the existence of a solidlike phase and provide an indication of the relative molecular dynamics of the C_α, C_β, and methyl group carbons. Figure 3 illustrates the variation in signal intensity with varying CP contact time. The observed rapid increase of signal intensity with lengthening CP contact time (a maximum occurs at ca. 500 μs) is indicative of strong dipolar interactions, i.e., solidlike, between carbon and hydrogen atoms. Continued signal growth is prevented by the decay of proton magnetization which is governed by $T_{1\rho}(^1H)$ relaxation. The CP experiments also reveal a high degree of rigidity in the peptide carbonyl carbon framework (160–200 ppm) since there is significant cross-polarization of the carbonyl carbon atom. This is noteworthy because of the absence of directly bonded protons. CSA broadening of the carbonyl signal makes quantification difficult. Figure 4 shows a typical CP spectrum of the aliphatic carbon region of lens proteins (0–100 ppm) with the fitted bands and their assignments.

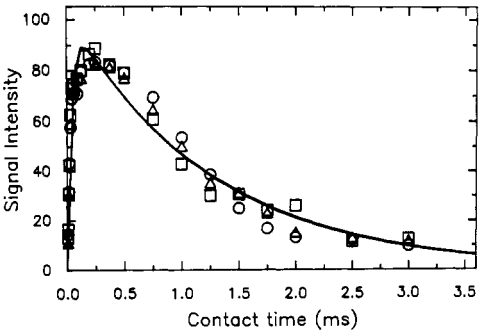

FIGURE 5: Cross-polarization signal intensity vs cross-polarization contact time for the C_α resonance of nuclear homogenate lens proteins at 1 °C (○), 20 °C (△), and 32 °C (□). The fitted lines are the nonlinear least-squares fits assuming the theoretical dependence by eq 1. Spectral acquisition parameters are noted under Experimental Procedures. Cross-polarization magnetization transfer parameters obtained by nonlinear regression are tabulated in Table I.

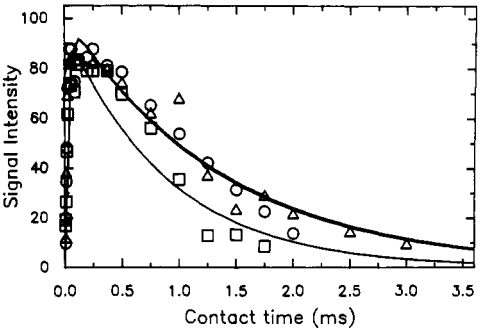

FIGURE 6: Cross-polarization signal intensity vs cross-polarization contact time for the C_β resonance of nuclear homogenate lens proteins at 1 °C (○), 20 °C (△), and 32 °C (□). The fitted lines are the nonlinear least-squares fits assuming the theoretical dependence by eq 1. Spectral acquisition parameters are noted under Experimental Procedures. Cross-polarization magnetization transfer parameters obtained by nonlinear regression are tabulated in Table I.

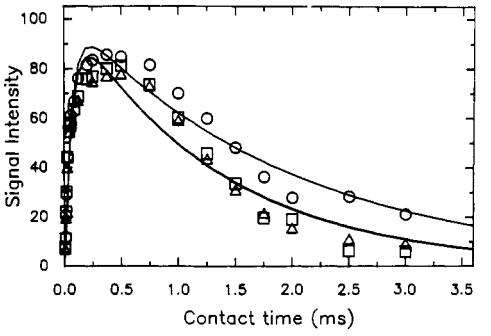

FIGURE 7: Cross-polarization signal intensity vs cross-polarization contact time for the C-methyl resonance of nuclear homogenate lens proteins at 1 °C (○), 20 °C (△), and 32 °C (□). The fitted lines are the nonlinear least-squares fits assuming the theoretical dependence expressed by eq 1. Spectral acquisition parameters are noted under Experimental Procedures. Cross-polarization magnetization transfer parameters obtained by nonlinear regression are tabulated in Table I.

The variable CP contact time experiments performed at 1, 20, and 32 °C (Figures 5–7) also provide insights into the molecular dynamics of the motionally restricted, or solidlike, lens proteins. The CP magnetization transfer parameters are tabulated in Table I. The protein polypeptide backbone chain α-carbons experience a restricted solidlike environment that

Table I: Cross-Polarization Magnetization Transfer Parameters for Native Calf Lens Nuclear Homogenate

resonance	T (°C)	H_{max} (% H_0)	$T_{1\rho}(^1H)$ (ms)	T_{CH} (μs)
C-Me	1	89 ± 4	2.0 ± 0.2	65 ± 7
C-Me	20	84 ± 6	1.3 ± 0.2	71 ± 12
C-Me	32	84 ± 6	1.3 ± 0.2	70 ± 11
C_β	1	91 ± 5	1.3 ± 0.2	30 ± 5
C_β	20	92 ± 5	1.4 ± 0.2	29 ± 5
C_β	32	87 ± 6	0.9 ± 0.1	38 ± 6
C_α	1	88 ± 5	1.2 ± 0.1	43 ± 6
C_α	20	89 ± 5	1.3 ± 0.1	40 ± 5
C_α	32	89 ± 4	1.3 ± 0.1	39 ± 4

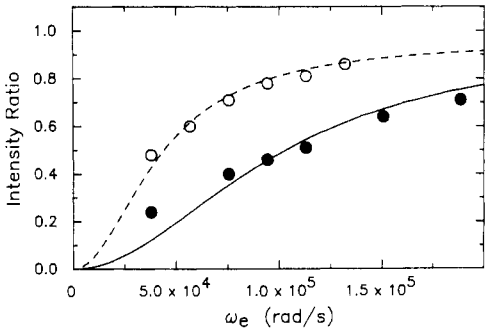

FIGURE 8: Carbonyl ^{13}C intensity ratio (R) vs ω_e plots for calf lens cortical homogenate protein at 35 °C (○) and 1 °C (●). The solid and dashed lines represent the best-fit lines obtained by nonlinear regression assuming a model of monodisperse isotropic reorientation with $\tau_{0,eff}$ values of 34 and 80 ns, respectively. Spectral acquisition parameters are noted under Experimental Procedures.

is essentially unchanged over the temperature range studied (Figure 5). Corresponding data for the side-chain β-carbons (Figure 6) suggest that their molecular environment is also hindered and essentially unchanged from 1 to 20 °C. However, at 32 °C, the molecular environment of the β-carbons becomes less hindered while still exhibiting solidlike cross-polarization characteristics. Protein methyl groups likewise demonstrate cross-polarization (Figure 7) but experience change in polarization transfer kinetic parameters [T_{CH}, $T_{1\rho}(^1H)$] upon a temperature change of 1 to 20 °C. No further change in these parameters occurs upon increasing the temperature to 32 °C.

As can be seen in Figures 5–7, the fitted lines using eq 1 do not duplicate the behavior of the data exactly. This fitting discrepancy may reflect nuclear protein domain heterogeneity of the solidlike phase and, hence, heterogeneity in $T_{1\rho}(^1H)$. However, the calculated curves are useful for semiquantitatively comparing overall trends.

Dilution of the nuclear homogenate from 42% protein (native) to 31% and 22% results in a decrease of the cross-polarization spectra intensity by ca. 70% and 85%, respectively. Little change occurs in cross-polarization kinetic parameters [T_{CH}, $T_{1\rho}(^1H)$] as reflected in data obtained from diluted samples vs data from the native sample taken at four different contact times (125, 250, 500, and 750 μs) (data not shown). Simple dilution does not affect the ability of the homogenate to display the intense light scattering associated with the cold cataract.

Cortical Homogenate. The carbonyl spectral intensity ratio frequency-dependent (dispersion) curves of the lens proteins present in a cortical homogenate obtained from an off-resonance rotating frame spin–lattice relaxation experiment at 35 and 1 °C are shown in Figure 8. The solid and dashed lines indicate the fitted theoretical frequency dispersion expected for a monodisperse collection of spherical tumbling macromolecules at the two temperatures with $\tau_{0,eff}$ times of 34 and 80 ns, respectively. As shown in Figure 8, the curves do not

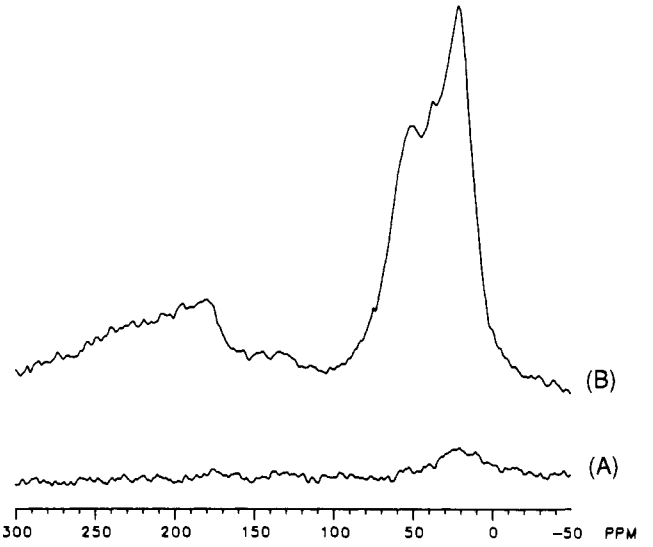

FIGURE 9: Cross-polarization ^{13}C NMR spectrum of calf lens homogenate protein at 20 °C. (A) Cortex; (B) nucleus. The contact time was 500 μs. Number of accumulations = 8000. A line-broadening factor of 150 Hz was applied to the FID prior to Fourier transformation. Other NMR parameters are listed under Experimental Procedures.

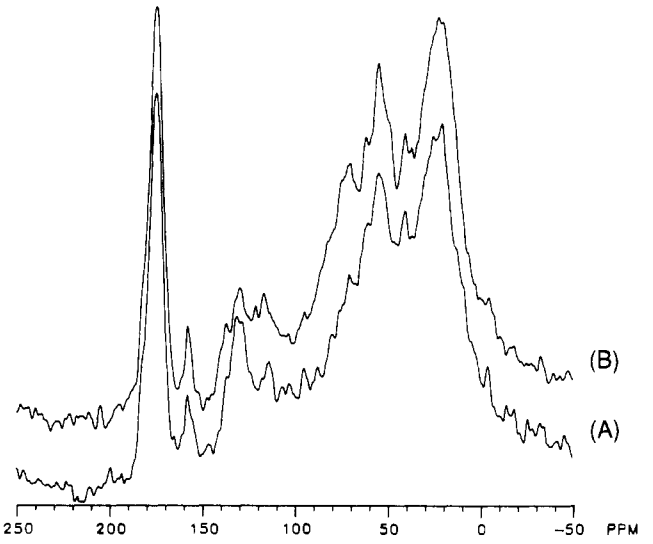

FIGURE 10: Comparison of ^{13}C NMR spectra of calf lens cortical homogenate proteins acquired in the presence and absence of proton dipolar decoupling at 1 °C: (A) scalar decoupled; (B) dipolar decoupled. Spectral acquisition parameters are noted under Experimental Procedures. Number of accumulations = 256. A line-broadening factor of 150 Hz was applied to the FID prior to Fourier transformation.

quite reach the limiting value of 1.00, as was the case with the nuclear homogenate; values of 0.96 are obtained at both temperatures. The 2.4-fold increase in τ_0 which accompanies a temperature change from 35 to 1 °C is in reasonable accord with the theoretically expected increase of 2.7-fold due to a decrease in temperature and an increase in temperature-induced solvent viscosity.

Cross-polarization NMR experiments performed on native cortical homogenate at 20 °C using the same spectral acquisition parameters employed for nuclear homogenate failed to yield significant CP signal intensity (Figure 9); for comparison, the corresponding nuclear homogenate CP spectrum is shown in Figure 9. However, ^{13}C NMR spectra of the proteins present in native cortical homogenate obtained in the presence of dipolar decoupling compared with the corresponding spectrum acquired under scalar decoupling conditions

Table II: Cross-Polarization Magnetization Transfer Parameters for Calf Lens Cortical Homogenate Concentrated to 42% Protein (Temperature = 20 °C)

resonance	H_{max} (% H_0)	$T_{1\rho}(^1H)$ (ms)	T_{CH} (μs)
C-Me	84 ± 5	1.0 ± 0.1	59 ± 8
C_β	89 ± 7	0.9 ± 0.1	29 ± 7
C_α	87 ± 4	0.8 ± 0.1	31 ± 4

at 1 °C show a small difference in spectral intensity (Figure 10). Spectral integration of the aliphatic region indicates that the fraction of solidlike material is 0.15. These results demonstrate that the cortical homogenate is predominantly mobile; i.e., the fraction of solidlike, or motionally restricted protein is low.

Variable contact time cross-polarization experiments at 20 °C performed on concentrated cortical samples (42% protein compared to 25% native) showed similar, but not identical, magnetization transfer kinetics to native nuclear homogenate (see Table II). The absolute signal intensity obtained from cross-polarization experiments of concentrated cortical homogenate is 50–70% less than the corresponding nuclear homogenate cross-polarization spectral intensity at CP contact times where maximum signal intensity is expected. Thus, a lower fractional content of solidlike material is indicated.

Polyacrylamide Gels. Polyacrylamide gels (5% cross-linking) with water contents ranging from 60% to 95% were also studied as models for the motional dynamics behavior of nuclear lens proteins. Off-resonance rotating frame ^{13}C measurements indicate substantial mobility of the side-chain carbonyls ($\tau_0 \approx 10^{-9}$ s). Gels with decreasing water content displayed increasingly broad ^{13}C carbonyl spectral line shapes, suggesting the occurrence of restricted polymer chain motion. Dipolar-decoupled ^{13}C NMR spectra show substantial intensity increases relative to the corresponding scalar-decoupled spectra as shown in Figure 11. For a gel of 79% water content, ca. 65% of the aliphatic carbons are engaged in slow polymer chain motion at 20 °C.

Variable contact cross-polarization experiments performed on polyacrylamide gels at 20 °C yield similar values of T_{CH} and $T_{1\rho}(^1H)$. When these two parameters are of the same magnitude, signal to noise suffers with a maximum possible signal of about 40% H_0 (Earl et al., 1987). Fitting the data also presents a problem in that the two time constants are highly correlated and are therefore indeterminant.

Discussion

The ^{13}C NMR results of this study establish the presence of both mobile and solidlike protein phases in calf lens nuclear homogenate, whereas for the native cortical homogenate, within the detection limits of the NMR technique, the protein phase is predominantly mobile.

Lens protein motional behavior, a reflection of molecular size and organization, has traditionally been investigated by the noninvasive technique of quasi-elastic light scattering which yields the translational mutual diffusion coefficient of the scattering particle (Tanaka & Benedek, 1975; Tanaka & Ishimoto, 1977; Nishio et al., 1984; Libondi et al., 1986; Latina et al., 1987; Benedek et al., 1987).

QELS studies of lens tissue have been interpreted in terms of two predominant classes of diffusing species, one slow and the other rapid. On the basis of the translational diffusion coefficient for purified α-crystallin (Andries et al., 1982), the more rapidly diffusing species was assigned to this protein, whereas the more slowly diffusing species, because of the calculated enormous size, approaching lens fiber cell dimensions, was simply referred to as an aggregated species. In the rabbit lens, the more slowly diffusing component was attributed to a gellike organization of the lens proteins (Libondi et al., 1986; Latina et al., 1987), while for the less dense human lens Benedek et al. (1987) proposed an aggregated form assembled from the more rapidly diffusing unaggregated species.

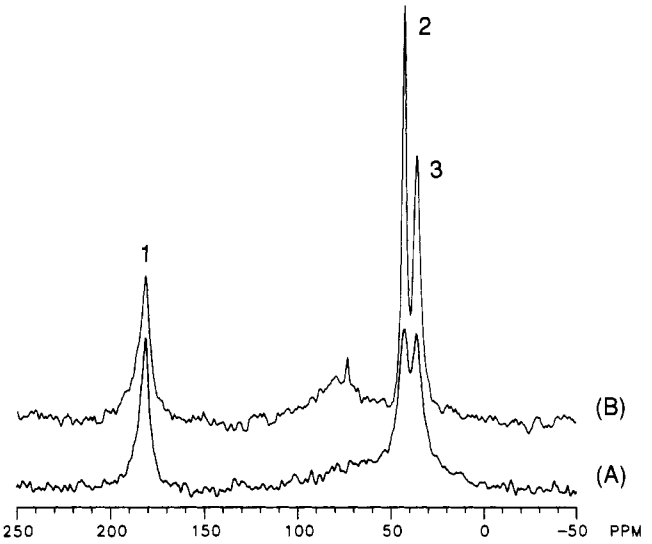

FIGURE 11: Comparison of ^{13}C NMR spectra of a polyacrylamide gel (5% cross-linking) containing 79% water acquired in the presence and absence of proton dipolar decoupling at 20 °C: (A) scalar decoupled; (B) dipolar decoupled. Spectral acquisition parameters are noted under Experimental Procedures. Number of accumulations = 64. A line-broadening factor of 100 Hz was applied to the FID prior to Fourier transformation. Resonance assignments: 1, carbonyl carbon; 2, CH; 3, CH_2.

Because of the square dependence of scattered light intensity on molecular weight, all of the QELS studies of lens cytoplasm failed to detect the lower molecular weight lens proteins, i.e., the β_H-, β_L-, LM-, and γ-crystallins, which constitute a sizable portion of the cytoplasmic water-soluble lens proteins. Only the presence of large proteins, such as α-crystallin and its aggregates, is detected.

Extensive lens protein purification and physical characterization studies (Siezen et al., 1979; Andries et al., 1982; Bindels et al., 1983; Harding & Crabbe, 1984) have established for the calf lens the following protein species in the cortex: α-crystallin, MW 780K, 40% of total soluble protein weight; β_H-crystallin, MW 100K–200K, 18% of total soluble protein; β_L-crystallin, MW 50K–80K, 27% of total soluble protein; LM- (β_S- and γ_H-) crystallin, MW 23K–28K, 6% of total soluble protein; γ_L-crystallin, MW 20K, 9% of total soluble protein. In contrast, nuclear lens proteins are somewhat larger: α-crystallin, MW 1100K, 35% of total soluble protein; β_H-crystallin, MW 110K–270K, 26% of total soluble protein; β_L-crystallin, MW 50K–80K, 11% of total soluble protein; LM- (β_S-) crystallin, MW 28K, 5% of total soluble protein; γ_L-crystallin, MW 20K, 23% of total soluble protein. Nuclear α-crystallin is also present in various oligomeric states, including a polymeric form composed of a branched three-dimensional network (Siezen et al., 1979). It is important to realize that such studies assess the aggregation state under assumed in vitro conditions, which probably does not realistically mirror the aggregation state in vivo. In addition, such studies also fail to characterize the water-insoluble fraction, which may be solubilized by sonication (Ortwerth et al., 1986). The major protein component of the water-insoluble fraction is α-crystallin (Ortwerth & Olesen, 1988).

The off-resonance rotating frame spin–lattice relaxation experiment is sensitive to rotational correlation times for molecular reorientation in the range of 1–500 ns (Schleich et

al., 1989). Assuming isotropic protein tumbling, a partial specific volume of 0.73 cm^3/g, an average hydration value of 0.51 g of H_2O/g of protein (Squire & Himmel, 1979), and the viscosity of pure water, a rotational correlation time of 400 ns is calculated for α-crystallin at 20 °C; Kerr effect birefringence measurements (Andries et al., 1982) give a value of 670 ns. Thus, the molecular reorientation of α-crystallin, as well as that of larger lens protein species, would not be expected to contribute significantly to the off-resonance rotating frame spin–lattice relaxation time measurements of lens homogenate proteins reported in this study.

The correlation time ($\tau_{0,eff}$) for lens protein rotational motion obtained by a nonlinear fit of R vs ω_e data is approximated (within 5%) by an average correlation time by $\sum g_i \tau_i^{a-1}$, where a is a constant having the value of 0.56 and g_i and τ_i are the weight fraction and rotational correlation time of the ith component, respectively, present in the mixture (Morgan et al., 1989). The observed value of $\tau_{0,eff}$ for lens proteins in the calf cortex at 35 °C is 34 ns. A precise theory linking the rotational correlation time for protein tumbling to concentration is lacking; however, it is known that τ_0 becomes longer with increasing protein concentration and may reflect solute-induced changes in solvent viscosity. It is also known that the apparent viscosity of cytoplasm is ca. 2–3 times that of pure water (Mastro & Keith, 1984; Mastro et al., 1984). Using the known polydispersity of the water-soluble lens cortical proteins (Bindels et al., 1983), and the definition of the average rotational correlation time obtained in the off-resonance rotating frame spin–lattice relaxation time experiment, we calculated a value for $\tau_{0,eff}$ of 33 ns assuming the protein parameters described above, and an apparent cytoplasmic viscosity 1.5 times that of pure water at the same temperature. Contributions, as noted above, from α-crystallin and larger aggregated protein species are not included. At 1 °C, the calculated mean value of 84 ns is in excellent agreement with the observed value of 80 ns for $\tau_{0,eff}$. Thus, the off-resonance rotating frame spin–lattice relaxation results are consistent with the known protein polydispersity of water-soluble lens proteins.

Similar calculations of the mean rotational correlation time for the proteins found in the nuclear region of the calf lens assuming an apparent cytoplasmic viscosity 3 times that of pure water yield a value of 64 ns, which is in close agreement with the measured value of 57 ns for $\tau_{0,eff}$. Reducing the temperature of the nuclear homogenate to 1 °C, a temperature below the cold cataract phase transition temperature (Clark & Benedek, 1980; Delaye et al., 1981, 1982), results in intense opacification and a observed $\tau_{0,eff}$ value of 43 ns, a value *smaller* than the 2.7-fold larger value predicted for this temperature decrease. The low temperature which produces the cold cataract could result in the elimination of the β_H- and LM-crystallin fractions, and possibly γ_s-crystallin as well, from the NMR-visible protein population, thus accounting for the decrease in $\tau_{0,eff}$.

QELS measurements of calf lens nuclear homogenates under conditions of clarity and cold cataract opacity are consistent with the presence of two motionally distinct classes of broadly distributed scatters with mean radii of 100 Å (α-crystallin) and 1500 Å (Delaye et al., 1982). The larger species, which corresponds to the aggregated form, is responsible for opacification associated with the cold cataract in the calf lens nucleus. This is supported by the observation that the concentration of the large species increases while the smaller species remains constant. These light-scattering results provide no information concerning the origin of the lens protein species responsible for the increased concentration of the larger aggregated form. The reduction in the mean value of the observed rotational correlation time for lens proteins attendant with cold cataract, and the analysis described above, suggests that β_H- and LM-crystallins and possibly γ_S-crystallin are the source of protein responsible for the increase in the fraction of the larger species. This interpretation is consistent with freeze–fracture electron microscopy studies of calf lens nuclear cytoplasm under cold cataract conditions (Gulik-Krzuicki et al., 1984) which reveal that the visualized segregated domains contain significant quantities of low molecular weight crystallins.

The off-resonance rotating frame spin–lattice relaxation NMR experiments provide measurements complementary to the light-scattering data by increasing the window of observation to the lower molecular weight proteins, thus affording insights into the motional dynamics of this class of crystallins in the lens.

To enable the detection, quantitation, and characterization of solidlike protein domains in lens cytoplasm, we have taken advantage of the differing ^{13}C NMR spectral characteristics of isotropically mobile and motionally restricted protein macromolecular species. Two different approaches have been utilized.

The spectral intensity of the resonances present in the ^{13}C spectra, recorded in the presence and absence of dipolar decoupling (Figure 2), clearly establishes the presence of a fraction of motionally restricted, i.e., solidlike, protein in the calf lens nucleus. The fraction of motionally restricted or solidlike material is 0.45 at 1 °C, 0.43 at 20 °C, and 0.35 at 35 °C. The carbonyl resonance region (160–200 ppm) displays a line width characteristic of a mixture of mobile and partially immobilized carbonyl carbons in both the dipolar and scalar-decoupled spectra. The solidlike fraction contributes a substantially broadened line width, the result of CSA relaxation and ^{13}C–^{14}N static dipolar effects, which are averaged out in the case of the mobile carbonyl carbons.

The suite of variable contact time ^{13}C cross-polarization spectra shown in Figure 3 are further evidence for the presence of solidlike protein domains in the lens nucleus. The maximum in the spectral intensity vs CP contact time curves for the different ^{13}C resonances present in the protein spectrum occurs at ca. 500 μs, indicating a rapid increase of ^{13}C cross-polarization spectral intensity with increasing contact time. The polymerized (gel) form of hemoglobin S, by contrast, has a maximum in spectral intensity at contact times greater than 1 ms, which indicates a less rigid solid than found for nuclear lens proteins. Of further importance is the substantial ^{13}C cross-polarization intensity observed for the peptide bond carbonyl carbon which has no directly attached protons. The variable contact time profiles for the major aliphatic resonance classes observed in the ^{13}C protein spectra recorded at different temperatures (Figures 5–7) provide insight into the motional dynamics of different parts of the protein structure. At all three temperatures studied, the polypeptide chain (C_α) backbone dynamics of lens proteins are similar and are representative of a rigid structure. For the side-chain C_β carbons, the dynamics are the same at 1 and 20 °C, whereas at 32 °C there appears to be a loosening of the side-chain environment. By contrast, the methyl group carbons experience substantially greater freedom at 20 and 32 °C than at 1 °C, where there appears to be less motional freedom. In all cases, the computed curves do not mirror precisely the experimental data points in the decay phase of the cross-polarization intensity. This may be a reflection of solid protein domain heterogeneity with

differing values of $T_{1\rho}(^1H)$. The solidlike protein domains persist upon dilution of the nuclear homogenate to a protein content reduced to at least 22%. The cross-polarization transfer rate and $T_{1\rho}(^1H)$ values are essentially invariant with dilution, indicating little change in protein structure dynamics.

For cortical homogenate, at its native protein content, an increase in ^{13}C spectral intensity of lens proteins is not observed at 20 °C upon dipolar decoupling, and, as expected, a significant ^{13}C cross-polarization spectrum is not obtained. However, at low temperature (1 °C), a small fraction (0.15) of solidlike phase is observed. When native cortical homogenate (25% protein) is concentrated to a protein concentration equivalent to that of the calf lens nuclear homogenate (42% protein), a ^{13}C lens protein CP spectrum is obtained. However, the absolute ^{13}C spectral intensity is 50–70% less than the corresponding CP spectrum obtained for nuclear material. The rapid buildup of CP spectral intensity is indicative of a rigid structure, thus illustrating the importance of molecular packing in defining protein mobility in concentrated protein environments. The CP magnetization transfer parameters for concentrated cortical homogenate proteins tabulated in Table II are indicative of a less rigid structure than displayed by the nuclear proteins. Moreover, the appearance of cross-polarizability at cortical lens protein concentrations characteristic of the nucleus may be related to the observation of the presence of a slowly relaxing component at high cortical protein concentrations in QELS experiments (Delaye & Gromiec, 1983). This slow relaxation time component may be related to the diffusion of aggregates, some of which may be nontouching, and thus, readily disappear upon dilution (Bauer, 1980).

Preliminary solid-state NMR studies of polyacrylamide gels reveal proton to carbon cross-polarization over a broad range of water contents, thus indicating the ability of a defined gel network to cross-polarize. The ease of preparing precisely defined polyacrylamide gels of known composition, cross-linking, and water content may provide an appropriate model system for lens protein gel studies.

As noted by Latina et al. (1987), three mechanisms may produce a change in the extent of lens protein interaction. These are as follows: (i) a change in molecular packing, achieved by changes in concentration; (ii) the formation of protein aggregates; and (iii) the process of gelation. These mechanisms are pertinent to the protein motional dynamics assessed by the NMR techniques employed in this study, which have a combined correlation time dynamic range exceeding 4 orders of magnitude. The off-resonance rotating frame spin–lattice relaxation studies and the scalar proton-decoupled spectral investigations clearly establish the presence of a mobile protein phase in both the lens cortex and nucleus. The presence of motionally restricted protein molecules (domains) can be accounted for either by aggregation, by gel formation, or by close molecular packing. The fact that substantial solidlike material is observed for a transparent lens nucleus, which does *not* disappear upon dilution, is suggestive of a gellike phase. To increase the rotational correlation time of α-crystallin to 10^{-5} s would require the association of at least 400 protein subunits of M_r 20K. Models of α-crystallin supramolecular organization containing up to 48 20K subunits have been proposed (Siezen et al., 1978; Siezen & Berger, 1978; Tardieu et al., 1986). This maximum value is inconsistent with the requirements imposed by cross-polarization. In turn, this suggests a more extensive, and hence rigid, quaternary structure for the proteins present in the nucleus, possibly a water-insoluble fraction, which does not occur in the cortex to any great extent at physiological temperature.

Nuclear magnetic resonance dispersion studies (Beaulieu et al., 1988) performed on calf lens nuclear homogenates at protein concentrations below 19% are consistent with the presence of a tumbling globular protein species of average molecular weight 700K, a value similar to that for α-crystallin. However, at protein concentrations greater than 19%, the characteristic NMRD inflection point of globular proteins is lost, suggesting a change in crystallin protein–protein interaction, and in turn organization. At high nuclear lens protein concentrations, the NMRD profiles resemble those of polymerized deoxy sickle hemoglobin (Lindstrom et al., 1976). It is interesting to note that the rotational correlation time for a protein, such as hemoglobin, contained within a gel is unaffected by the gel network (Lindstrom & Koenig, 1974).

The NMR studies presented here reveal a significant difference between the structure, organization, and motional behavior of the lens proteins of the nucleus and cortex. This finding undoubtedly has a bearing on the numerous biochemical and biophysical differences observed for the cortex and nucleus.

Acknowledgments

We thank Dr. Richard Wittebort for sugggestions regarding high-power probe design and Dr. Wanda F. Williams and Dane Travis for help with preliminary off-resonance rotating frame spin–lattice relaxation measurements.

References

Alemany, L. B., Grant, D. M., Pugmire, R. J., Alger, T. D., & Zilm, K. W. (1983) *J. Am. Chem. Soc. 105*, 2133–2141.
Andries, C., Backhovens, H., Clauwaert, J., de Block, J., de Voeght, F., & Dhont, C. (1982) *Exp. Eye Res. 34*, 239–255.
Bauer, D. R. (1980) *J. Chem. Phys. 84*, 1592–1598.
Beaulieu, C. F., Clark, J. I., Brown, R. D., III, Spiller, M., & Koenig, S. H. (1988) *Magn. Reson. Med. 8*, 45–57.
Benedek, G. B., Chylack, L. T., Jr., Libondi, T., Magnante, P., & Pennett, M. (1987) *Curr. Eye Res. 6*, 1421–1432.
Bindels, J. G., Bessems, G. J. J., de Man, B. M., & Hoenders, H. J. (1983) *Comp. Biochem. Physiol. 76B*, 47–55.
Bloch, F. (1958) *Phys. Rev. 111*, 841–853.
Carper, D., Russel, P., Shinohara, T., & Kinoshita, J. H. (1985) *Exp. Eye Res. 40*, 85–94.
Clark, J. I., & Benedek, G. B. (1980) *Biochem. Biophys. Res. Commun. 95*, 482–489.
Daniel, C., & Wood, F. S. (1980) *Fitting Equations to Data*, 2nd ed., Wiley, New York.
Delaye, M., & Gromiec, A. (1983) *Biopolymers 22*, 1203–1221.
Delaye, M., & Tardieu, A. (1983) *Nature 302*, 415–417.
Delaye, M., Clark, J. I., & Benedek, G. B. (1981) *Biochem. Biophys. Res. Commun. 100*, 908–914.
Delaye, M., Clark, J. I., & Benedek, G. B. (1982) *Biophys. J. 37*, 647–656.
Demco, D. E., Tegenfeldt, J., & Waugh, J. S. (1975) *Phys. Rev. B11*, 4133–4151.
Earl, W. L., & VanderHart, D. L. (1982) *J. Magn. Reson. 48*, 35–54.
Earl, W. L., Wershaw, R. L. & Thorn, K. A. (1987) *J. Magn. Reson. 74*, 264–274.
Farnsworth, P. N., Shyne, S. E., Caputo, S., Fassano, A. V., & Spector, A. (1978) *Exp. Eye Res. 30*, 611–615.
Gerstein, B. C., & Dybowski, C. R. (1985) *Transient techniques in NMR of solids*, Academic Press, Orlando, FL.
Gulik-Krzywicki, T., Tardieu, A., & Delaye, M. (1984) *Biochim. Biophys.* Acta *800*, 28–32.
Haner, R. L., Schleich, T., Morgan, C. F., & Rydzewski, J.

M. (1989) *Exp. Eye Res.* (in press).
Harding, J. J., & Crabbe, M. J. C. (1984) in *The Eye* (Davson, H., Ed.) 3rd ed., Vol. 1b, pp 207–492, Academic Press, London.
Hartmann, S. R., & Hahn, E. L. (1962) *Phys. Rev. 128*, 2042–2053.
James, T. L. (1984) in *Phosphorus-31 NMR, Principles and Applications* (Gorenstein, D. G., Ed.) pp 349–400, Academic Press, New York.
James, T. L., Matson, G. B., Kuntz, I. D., Fisher, R. W., & Buttlaire, D. H. (1977) *J. Magn. Reson. 28*, 417–426.
James, T. L., Matson, G. B., & Kuntz, I. D. (1978) *J. Am. Chem. Soc. 100*, 3590–3594.
James, T. L., Mathews, R., & Matson, G. B. (1979) *Biopolymers 18*, 1763–1768.
Jiang, Y. J., Pugmire, R. J., & Grant, D. M. (1987) *J. Magn. Reson. 71*, 485–494.
Latina, M., Chylack, L. T., Jr., Fagerholm, P., Nishio, I., Tanaka, T., & Palmquist, B. M. (1987) *Invest. Ophthalmol. Visual Sci. 28*, 175–183.
Libondi, T., Magnante, P., Chylack, L. T., Jr., & Benedek, G. B. (1986) *Curr. Eye Res. 5*, 411–419.
Lindstrom, T. R., & Koenig, S. H. (1974) *J. Magn. Reson. 15*, 344–353.
Lindstrom, T. R., Koenig, S. H., Boussios, T., & Bertles, J. F. (1976) *Biophys. J. 16*, 679–689.
Lyerla, J. R., Yannoni, C. S., & Fyfe, C. A. (1982) *Acc. Chem. Res. 15*, 208–216.
Mastro, A. M., & Keith, A. D. (1984) *J. Cell Biol. 99*, 180s–187s.
Mastro, A. M., Babich, M. A., Taylor, W. D., & Keith, A. D. (1984) *Proc. Natl. Acad. Sci. U.S.A. 81*, 3414–3418.
Matson, G. B., Schleich, T., Serdahl, C. Acosta, G., & Willis, J. A. (1984) *J. Magn. Reson. 56*, 200–206.
McEwan, J. R., & Farnsworth, P. N. (1987) *Exp. Eye Res. 44*, 567–576.
Mehring, M. (1983) *Principles of High Resolution NMR in Solids*, 2nd ed., pp 151–168, Springer-Verlag, New York.
Morgan, C. F., Schleich, T., & Caines, G. H. (1989) *Biopolymers* (in press).
Neville, M. C., Paterson, C. A., Rae, J. L., & Woessner, D. E. (1974) *Science 184*, 1072–1074.
Nishio, I., Weiss, J. N., Tanaka, T., Clark, J. I., Giblin, F. G., Reddy, V. N., & Benedek, G. B. (1984) *Exp. Eye Res. 39*, 61–68.
Ortwerth, B. J., & Olesen, P. R. (1988) *Invest Ophthalmol. Visual Sci. (ARVO Suppl.) 29*, 185.
Ortwerth, B. J., Olesen, P. R., & Sharma, K. K. (1986) *Exp. Eye Res. 43*, 955–963.
Philipson, B. T., & Fagerholm, P. P. (1973) *Ciba Found. Symp. 19*, 45–63.
Pines, A., Gibby, M. G., & Waugh, J. S. (1973) *J. Chem. Phys. 59*, 569–590.
Schaefer, J., Stejskal, E. O., & Buchdahl, R. (1977) *Macromolecules 10*, 384–405.
Schleich, T., Morgan, C. F., & Caines, G. H. (1989) *Methods Enzymol.* (in press).
Siezen, R. J., & Berger, H. (1978) *Eur. J. Biochem. 91*, 397–405.
Siezen, R. J., Bindels, J. G., & Hoenders, H. J. (1978) *Eur. J. Biochem. 91*, 387–396.
Siezen, R. J., Bindels, J. G., & Hoenders, H. J. (1979) *Exp. Eye Res. 28*, 551–567.
Stejskal, E. O., & Schaefer, J. (1975) *J. Magn. Reson. 18*, 560–563.
Sutherland, J. W. H., Egan, W., Schechter, A. N., & Torchia, D. A. (1979) *Biochemistry 18*, 1797–1803.
Tanaka, T. (1978) *Phys. Rev. Lett. 40*, 820–823.
Tanaka, T., & Benedek, G. B. (1975) *Invest. Ophthalmol. 14*, 449–456.
Tanaka, T., & Ishimoto, C. (1977) *Invest Ophthalmol Visual Sci. 16*, 135–140.
Tardieu, A., Laporte, D., Licinio, P., Krop, B., & Delaye, M. (1986) *J. Mol. Biol. 192*, 711–724.
Torchia, D. A., & VanderHart, D. L. (1979) in *Topics in Carbon-13 NMR Spectroscopy* (Levy, G. C., Ed.) Vol. 3, pp 325–360, Wiley, New York.
Yannoni, C. S. (1982) *Acc. Chem. Res. 15*, 201–208.
Zigler, J. S., Jr., & Goosey, J. (1981) *Trends Biochem. Sci. (Pers. Ed.) 6*, 133–136.